Separation Science and Technology
Publication details, including instructions for authors and subscription information:
http://www.informaworld.com/smpp/title~content=t713708471

Adsorption Behavior of Anionic Reactive Dyes on H-type Activated Carbon: Competitive Adsorption and Desorption Studies

Musa I. El-Barghouthi[a]; Amjad H. El-Sheikh[a]; Yahya S. Al-Degs[a]; Gavin M. Walker[b]
[a] Chemistry Department, The Hashemite University, Zarqa, Jordan [b] School of Chemistry and Chemical Engineering, Queen's University Belfast, Belfast, UK

To cite this Article El-Barghouthi, Musa I. , El-Sheikh, Amjad H. , Al-Degs, Yahya S. and Walker, Gavin M.(2007) 'Adsorption Behavior of Anionic Reactive Dyes on H-type Activated Carbon: Competitive Adsorption and Desorption Studies', Separation Science and Technology, 42: 10, 2195 — 2220

To link to this Article: DOI: 10.1080/01496390701444030

URL: http://dx.doi.org/10.1080/01496390701444030

Separation Science and Technology, 42: 2195–2220, 2007
Copyright © Taylor & Francis Group, LLC
ISSN 0149-6395 print/1520-5754 online
DOI: 10.1080/01496390701444030

Adsorption Behavior of Anionic Reactive Dyes on H-type Activated Carbon: Competitive Adsorption and Desorption Studies

Musa I. El-Barghouthi, Amjad H. El-Sheikh,
and Yahya S. Al-Degs
Chemistry Department, The Hashemite University, Zarqa, Jordan

Gavin M. Walker
School of Chemistry and Chemical Engineering, Queen's University
Belfast, Belfast, UK

Abstract: A microporous H-type activated carbon was shown to be effective for removing anionic reactive dyes from single and binary component solutions. The extent of the dye adsorption from a single-solute solution was high (0.25–0.42 mmol/g). From the binary dye solutions, the experimental data indicated a high degree of competition for active sites and the obtained adsorption capacities were reduced to 0.10–0.26 mmol/g. Adsorption data from single dye solutions were correlated using the Langmuir, Ferundlich, and Redlich-Peterson models. Hydrophobic, hydrophobic mechanisms were significant in the adsorption process. Furthermore, the system showed a low extent of desorption.

Keywords: Reactive dyes, adsorption, microporosity, competitive adsorption, K_{OW}, hydrophobic-hydrophobic interactions, desorptions

INTRODUCTION

Waste effluent from the textile industry can be particularly problematic due to the presence of color in the final effluent. This color, on entering the water

Received 3 August 2007, Accepted 16 April 2007

Address correspondence to Gavin M. Walker, School of Chemistry and Chemical Engineering, Queen's University Belfast, Belfast BT9 5AG, UK. Tel.: +44(0)28 9097 4172; Fax: +44(0)28 9097 4627; E-mail: g.walker@qub.ac.uk

systems, is highly visible and thus undesirable. Currently, reactive dyes are one of mostly used classes of dye in the textile industry (1). Reactive dyes utilize a chromophore containing a substituent that is capable of directly reacting with the fibre substrate. The strong covalent bonds that attach reactive dye to fibers make it among the most permanent of dyes. “Cold” reactive dyes, such as Procion MX, Cibacron F, Levafix Brilliant, and Drimarene K, are very easy to use because the dye can be applied at room temperature. Due to their strong interaction with many surfaces of synthetic and natural fabrics, reactive dyes are highly used for coloring a wide range of materials including wool, cotton, nylon, silk, and modified acrylics (2). Discharging of dyes into the hydrosphere is problematic because dyes gave water an undesirable color (3) also reducing the photosynthetic reactions by inhibiting sunlight penetrations; furthermore, some dyes are known to be toxic and carcinogenic (4).

Recently, research on wastewater treatment has been directed to the elimination of reactive dyes for mainly three reasons. First, reactive dyes represent 20 to 30% of the total dyes market (5). Second, a large fraction of reactive dyes (10–50%) are wasted during the dyeing process (6). Third, conventional wastewater treatment methods, which rely on oxidation and aerobic biodegradation, were found to be inefficient for complete elimination of reactive dyes (1). Current methods used for elimination of reactive dyes from wastewater can be classified into physical, chemical, and biological methods (7). Even though the chemical and biological methods are effective for removing dyes, they require special types of equipment and usually consume more energy. In addition, large amounts of by-products result from these methods (1). Physical methods which include adsorption, ion-exchange, and membrane filtration are effective for removing reactive dyes and have many advantages compared to the other existing methods (7). Adsorption of cationic and anionic dyes by activated carbon and by a number of natural adsorbents has been investigated in literature (8, 9). Anionic reactive dyes have a modest adsorption extent on a wide range of natural and synthetic adsorbents; therefore, several attempts were made to search for adsorbents of high adsorption capacity for this type of dye. Activated carbons usually outperformed most adsorbents in removing reactive dyes from solution. Activated carbons generally have a high adsorption capacity for anionic reactive dyes, cationic dyes, and many other organic pollutants (10). Within literature, numerous research papers considered the adsorption of reactive dyes from single-solute solution, however, relatively few papers considered the adsorption of reactive dyes from multi-solute solution systems (11, 12). In addition, few studies have considered the desorption behavior of reactive dyes (13). Hence, this study was undertaken to address the problems associated with the adsorption of reactive dyes from multi-component solutions and to investigate the extent of desorption of reactive dyes from activated carbon. In this work, two problematic anionic reactive dyes (Levafix Brilliant Red E-4BA and Levafix Brilliant Blue E-4BA) were removed from synthetic dye solutions using a highly porous activated carbon having a large surface area. Adsorption isotherms of reactive dyes from single and bi-solute systems were conducted at the following conditions: concentration range: $0-1.2 \times 10^{-3}$ mol dm^{-3}, pH 5.5, temperature 25.0°C, and zero ionic strength. Adsorption isotherms of reactive dyes from single and bi-solute systems were correlated to a number of models including Langmuir, Ferundlich, Redlich-Peterson, and competitive-Langmuir models. The *n*-octanol/water partition coefficient (K_{OW}) value of reactive dyes was investigated to determine the nature of interaction between dyes and activated carbon. Desorption of reactive dyes by water was also investigated at 25°C to determine the fraction of reversible and irreversible fractions of adsorbed dye.

EXPERIMENTAL

Adsorbent and Adsorbates

Activated carbon adsorbent was purchased from Calgon, A.C. company (Pittsburgh, Pennsylvania, USA). The adsorbent was used as obtained from manufacturers without any chemical or physical treatment (particle diameter 300–500 μm). The bulk density and the porosity of the adsorbent were given by the manufacturer, 0.64 g cm^{-3} and 0.4 respectively.

Two reactive dyes of industrial application were studied; namely, Levafix Brilliant Red E-4BA ($C_{29}H_{19}O_{11}N_7S_3ClNa_3$), and Levafix Brilliant Blue E-4BA ($C_{31}H_{19}O_9N_5S_2Cl_2Na_2$). Throughout the text, Levafix Brilliant Red E-4BA and Levafix Brilliant Blue E-4BA were referred to as red dye and blue dye respectively. Reactive dyes of purity more than 99% (wt/wt) were obtained from the manufacturer directly (Bayer, Frankfurt, Germany). The stock solutions of dyes that were used in the adsorption experiments were prepared from their corresponding pure dried solid materials. The dyes are highly soluble in water, their solubility according to the manufacturer are 100 and 60 g/dm^3 for the blue and the red dye respectively. The wavelengths of maximum absorption for the dyes were 513.0 and 596.0 nm for red and blue dye respectively. The structures showing a minimum energy for free dye molecules were predicted by the semiempirical molecular orbital method (PM3 method) (14). The PM3 method was undertaken using the Hyperchem version 6 package (Hypercube, Inc., Gainesville, FL). The chemical structures of dyes with their real dimensions as predicted from the Hyperchem program are shown in Fig. 1.

Chemical and Physical Characteristics of Activated Carbon

The Boehm titration method is widely used to determine the acidic and basic surface groups of activated carbons (15). In the Boehm titrations, 25 cm^3 of

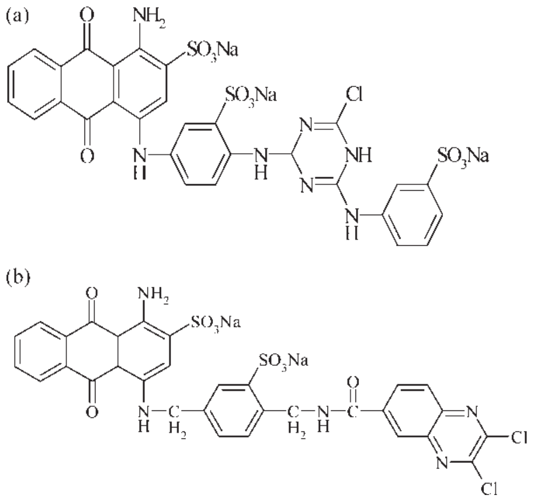

Figure 1. Chemical structure of reactive dye molecules. a) Levafix Brilliant Red E-4BA. (molar mass = 841.5 g/mol, molecular dimensions 1.92 and 1.25 nm). b) Levafix Brilliant Blue E-4BA. (molar mass = 786.0 g/mol, molecular dimensions 2.20 and 1.10 nm).

either 0.05 M HCl solution, NaOH solution, Na_2CO_3 solution or $NaHCO_3$ solution were added separately to dried samples of activated carbon (0.500 ± 0.001 g). The samples were agitated for 24 hours and the excess acid or base in 5.0 cm^3 of the filtrate was titrated with 0.05 M HCl or NaOH. Surface acidity or basicity was calculated based on the assumption that $NaHCO_3$ neutralized carboxyl groups only, Na_2CO_3 neutralized carboxyl and lactonic groups, NaOH neutralized all acidic groups including carboxyl, lactonic, and phenolic groups, and HCl neutralized all the basic groups. The textural characteristics of activated carbon including the surface area, the pore volume, the pore size distribution, and other characteristics were determined using N_2–adsorption techniques (Nova 4200e, Surface Area and Pore Size Analyzer). A sample of activated carbon (0.200 ± 0.001 g) was degassed overnight at 300°C prior to N_2 adsorption. In analysis of N_2 adsorption data, the cross-sectional area of N_2 molecule was taken as 16.2 $Å^2$ (16).

Adsorption Isotherm of Reactive Dyes from Single and Bi-solute Solutions

Equilibrium isotherms for single and binary mixtures were carried out at 25 ± 1°C, whereby 0.200 (±0.001) g of activated carbon of particle diameter range (300–500 μm) was added to 250 cm^3 glass bottles containing 100.0 cm^3 of reactive dye of varying concentration ($0–1.2 \times 10^{-3}$ mol dm^{-3}).

The bottles were sealed and placed in a thermostated shaker (GFL 1083, Germany) for two weeks to attain equilibrium. The initial pH of dye solutions was measured using a digital pH meter (WTW, inolab, Germany) and was found to be in the range 5.0–5.5. The equilibrium time for dye adsorption on activated carbon was determined previously and it was found that a two-week period was sufficient for dyes to attain equilibrium. After two weeks of constant shaking, the samples were removed, filtered through 0.45 μm Millipore cellulose nitrate filters, and subsequently analyzed to measure the equilibrium concentration of dye using a spectrophotometer (Cary 50 UV-Vis spectrophotometer). Linear calibration graphs (absorbance vs concentration) were obtained and the dynamic range for both dyes was:0.01– 80.0 ppm. The equilibrium concentration of dyes was determined by converting the optical densities to concentration using a pre-determined linear calibration graph for each dye. The amount of dye adsorbed was calculated from the difference between the initial and final concentration remaining in the solution after equilibrium. The initial concentration range of each dye was set at $0 - 1.2 \times 10^{-3}$ mol dm^{-3} in a bi-solute solution while keeping the other experimental conditions similar to those in single-solute systems.

For each isotherm system, an experiment without the adsorbent was performed in parallel to test the possible adsorption of dyes onto the container walls. The results showed that dye adsorption onto the container walls and to the Millipore cellulose nitrate filters were negligible. Adsorption isotherm experiments were repeated in duplicate and the average values are reported.

The concentration of dyes in bi-solute solution was estimated using the modified Beer's law for a solution containing two absorbing species (17). The concentration of blue and red dye in a mixture was determined by measuring the absorbance of the mixture at the maximum wavelength of each dye. The absorbances of the mixture measured at the maximum wavelength of each dye can be presented as follows:

$$A_{513} = \varepsilon_{\mathrm{red}(513)} b C_{\mathrm{red}} + \varepsilon_{\mathrm{blue}(513)} b C_{\mathrm{blue}} \tag{1}$$

$$A_{596} = \varepsilon_{\mathrm{red}(596)} b C_{\mathrm{red}} + \varepsilon_{\mathrm{blue}(596)} b C_{\mathrm{blue}} \tag{2}$$

Where A_{513}, A_{596}, $\varepsilon_{\mathrm{red}(513)}$, $\varepsilon_{\mathrm{blue}(513)}$, $\varepsilon_{\mathrm{red}(596)}$, $\varepsilon_{\mathrm{blue}(596)}$, b, C_{red} and C_{blue} are: absorbance of dye mixture at 513 nm, absorbance of dye mixture at 596 nm, the molar absorptivity of the red dye at 513 nm, the molar absorptivity of the blue dye at 513 nm, the molar absorptivity of the red dye at 596 nm, the molar absorptivity of the blue dye at 596 nm, the bath length of absorbing medium (cm), the molar concentration of the red dye, and the molar concentration of the blue dye respectively. The four molar absorptivities were determined for reactive dyes as follows. For the blue dye, ten solutions were prepared covering the concentration range: 5.0–70.0 ppm. The absorbance of each solution was measured at 596 nm and 513 nm. Two plots were generated using Beer's law ($A = \varepsilon bC$), first one is the plot for measurements at 596 nm and the second plot is for measurements at 513 nm. As $b = 1$ cm, then the slope of the first plot is equal to the molar absorptivity of blue dye at 596 nm and slope of the second plot is equal to the molar absorptivity (ε) of blue dye at 513. A similar procedure was carried out for the red dye. The values of the molar absorptivity of dyes at 596 and 513 nm were: $\varepsilon_{\text{blue}(596)} = 5500$, $\varepsilon_{\text{blue}(513)} - 1500$, $\varepsilon_{\text{red}(513)} = 13900$, and $\varepsilon_{\text{red}(596)} = 325\ \text{L mol}^{-1}\ \text{cm}^{-1}$.

Determination of Octanol/Water Partition Coefficient (K_{OW}) of Reactive Dyes

The partition coefficient (K_{OW}) of reactive dyes between *n*-octanol and water was determined at 25°C by a shake-flask method as described in the literature (18). Partitioning experiments of dyes were carried out at 15:100 (V/V ratio) of *n*-octanol (99% purity) and distilled water. A 100.0 cm^3 of dye solution (0.20 M) was prepared in a 250 cm^3 flask. To this solution, a 15 cm^3 of *n*-octanol is added and the mixture is sealed and placed in the thermostated shaker for 24 hours to ensure equilibrium. After centrifugation of the mixture at a speed of 2000 rpm, the aqueous phase was separated and the amount of dye in this phase is determined using the spectrophotometer. The partition coefficient (K_{OW}) of the dye can be estimated from the following relation (18).

$$K_{OW} = \frac{C_{oct}}{C_{aq}} \tag{3}$$

Where C_{oct} is the equilibrium dye concentration in the organic layer and C_{aq} is the corresponding dye concentration remaining in the aqueous phase. The amount of dye that transfers to the octanol phase was taken as the difference between the initial (0.20 M) and final dye concentration in the aqueous phase. The accuracy of this procedure was checked by analysing the octanol phase and then checking the transfer by mass balance.

Desorption Experiments

Desorption of adsorbed dyes was determined by adding 0.200 ± 0.001 g of activated carbon of a particle diameter range (300–500 μm) to 250 cm^3 glass bottles containing 100 cm^3 of reactive dye of varying concentration ($0 - 1.2 \times 10^{-3}\ \text{mol dm}^{-3}$). The bottles were sealed and placed in a thermostated shaker for two weeks. After attainment of equilibrium, the remaining dye concentration was quantified using the spectrophotometer. The activated carbon was separated from the dye solution and rinsed several times with distilled water to remove any free dye. Each bottle was then refilled with 100.0 cm^3 of distilled water and the bottles were sealed and shaken for two weeks to ensure equilibration. Then 5 to 10 mL sample of each solution was removed and filtered through 0.45 μm Millipore cellulose nitrate filters and subsequently analyzed to measure the concentration of the desorbed dye using the spectrophotometer.

RESULTS AND DISCUSSION

Characterization of the Adsorbent

Chemical Characteristics

The total surface functional groups and $pH_{solution}$ are important characteristics for any activated carbon, as such characteristics can indicate the acidity/basicity, the type of adsorbent (either H or L-type), and the net surface charge of the carbon aqueous solution.

Table 1 summarizes the results of the Boehm's titration experiment. The results in Table 1 indicate that the activated carbon has both basic and acidic properties. Acid functional groups are: carboxylic, lactonic, and phenolic (19). The basic functional groups include oxygen-containing species such as ketonic, pyronic, chromenic, and π-electron system of carbon basal planes (19, 20). The activated carbon has more basic properties and a modest density of surface functional groups (0.54 group/nm^2). A value of 14.9 group/nm^2 was reported for some activated carbons (19). The density of surface functional groups depends on the preparation conditions and on the nature of the precursor of the activated carbon (21). Due to their importance in the attraction of polar-solutes from solution, many chemical treatment procedures are employed to increase the density of surface functional groups of activated carbons (22).

The type of activated carbon employed in this work is the H-type according to the Mattson and Mark classification of activated carbons (21).

Table 1. Acidity/basicity and $pH_{solution}$ of activated carbon[a]

Total basic groups (mmol/g)	0.43
Total acidic groups (mmol/g)	0.30
Carboxylic groups (mmol/g)	0.06
Lactonic groups (mmol/g)	0.08
Phenolic groups (mmol/g)	0.16
Total functional groups (mmol/g)	0.73
Density of groups on the surface (group/nm^2)[b]	0.54
$pH^{c}_{solution}$	9.1

[a] All the reported results are averaged of three experiments.

[b] Specific surface area = 820 m^2/g.

[c] $pH_{solution}$ was obtained as follows: 1.0 g of dried carbon is added to 10.0 mL of degassed distilled water and agitated for 24 h then the pH of the mixture was recorded (23).

When added to distilled water, the H-carbon gives a basic solution and a protonated surface, while the L-carbon has an acidic solution and a deprotonated surface. Accordingly, the H-type activated carbons are effective adsorbents for reactive dyes due to the high electrostatic attraction between negatively charged molecules of reactive dyes (due to presence of sulphonate groups, see Fig. 1) and positively charged H-activated carbon (23).

Physical Characteristics

The textural characteristics of activated carbon obtained from N_2-adsorption studies are summarized in Table 2. As indicated (in Table 2), the adsorbent has a relatively large specific surface area (820 m^2/g) which is typical for commercial activated carbons (24–28). Comparing the magnitude of the total surface area with the surface area of micropores indicates the high microporosity of the adsorbent with the surface area of the micropores contributing 86% of the total surface area. The large microporosity of the adsorbent is also evident when comparing the micropore volume with the total pore volume of the adsorbent with the micropore volume contributing to about 82% of the total pore volume. The percentage of microporosity can be further increased using chemical procedures; the percentage of microporosity can be increased to 99% for activated carbon after treatment by NaOH solution (29). Typically, pores of activated carbon can be divided into micropores with a pore diameter of less than 2 nm, mesopores with pore diameter range between 2–50 nm, and the large macropores of a pore diameter of more than 50 nm (28). As illustrated in Fig. 2, the average pore diameter of the adsorbent is 1.8 nm as obtained from Barrett-Joyner-Hanlenda (BJH) method (24) which indicates that the adsorbent is highly microporous.

Table 2. Textural characteristics of activated carbon

S^a_{BET} (m^2/g)	820
$S^b_{external}$ (m^2/g)	110
S^c_{mic} (m^2/g)	710
Total pore volume^d (cm^3/g) (V_{tot})	0.56
Micropore (diameter $<$ 2 nm) volume^e (cm^3/g)	0.46
Mesopore (diameter: 2–50 nm) volume^f (cm^3/g) (V_{mes})	0.10
Average pore diameterg (nm)	1.8

[a] Specific surface area (multipoint BET method (24)).

[b] External surface area (t-plot method (24)).

[c] Micropore surface area (t-plot method (24)).

[d] Calculated from the amount of N_2 adsorbed at $P/P_0 = 0.95$ (25).

[e] Obtained from Dubinin-Radushkevich method (16).

[f] Calculated from the amount of N_2 adsorbed between relative pressure P/P_0: 0.40–0.95 assuming that molar volume of liquid nitrogen is 35 $cm^3\ mol^{-1}$ (26).

[g] Obtained from Barrett-Joyner-Hanlenda (BJH) method (24).

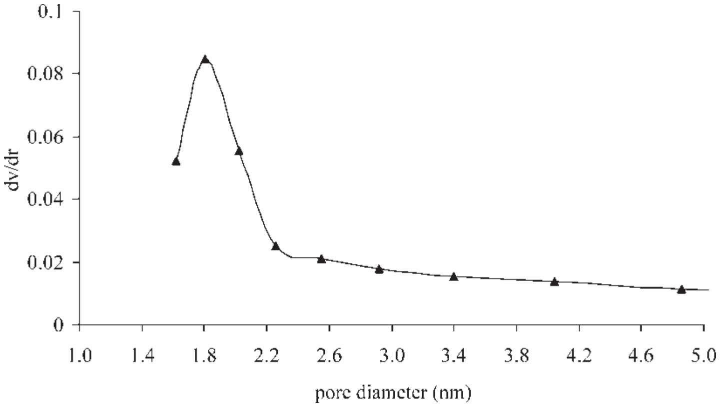

Figure 2. Pore size distribution of the adsorbent according to Barrett-Joyner-Hanlenda (BJH) method.

Adsorption Isotherms of Dyes by Activated Carbon

Adsorption isotherms of reactive dyes from single and bi-solute solutions using activated carbon are shown in Fig. 3. The shape of dye adsorption isotherms in single and bi-solute solutions indicates that these isotherms are of L2-isotherm according to Giles classification for isotherms (30). In L2-isotherms, adsorption of solute on the adsorbent proceeds until a monolayer is established and the formation of more than one layer is not possible (30). The shape of isotherms presented in Fig. 3 a and b is indicative of a very high affinity between the adsorbent surface and the dyes. For both dyes, the carbon effectively removes the dyes at lower initial concentrations; the isotherms then reach a maximum capacity as indicated by the plateau of the data.

Moreover, the majority of reported adsorption isotherms of reactive dyes have feature of L2-isotherm type behaviour (4, 31–33). L2-isotherm type (or some times called Langmuir isotherm type) is usually associated with ionic solute (e.g., metal cations and ionic dyes) adsorption with weak competition from the solvent molecules (30). Accordingly, the anionic reactive dye molecules favorably adsorb on the carbon surface with low competition from water molecules and the dye adsorption continues until the surface concentration reaches a maximum value. The formation of more than one layer is not possible due to the electrostatic repulsion between adsorbed dyes molecules and those in solution.

The correlation of the experimental adsorption data of reactive dyes from single and bi-solute solutions with a number of adsorption models was made to gain an insight into the adsorption behavior of dyes from solution and to determine the heterogeneity of the surface of the activated carbon.

Two-Parameter Models

Two of the most commonly used isotherm models have been used in this work, namely, the Langmuir and Freundlich models. The form of the Langmuir equation can be represented as follows (34).

$$q_e = \frac{Q_{\max} K_L C_e}{1 + K_L C_e} \tag{4}$$

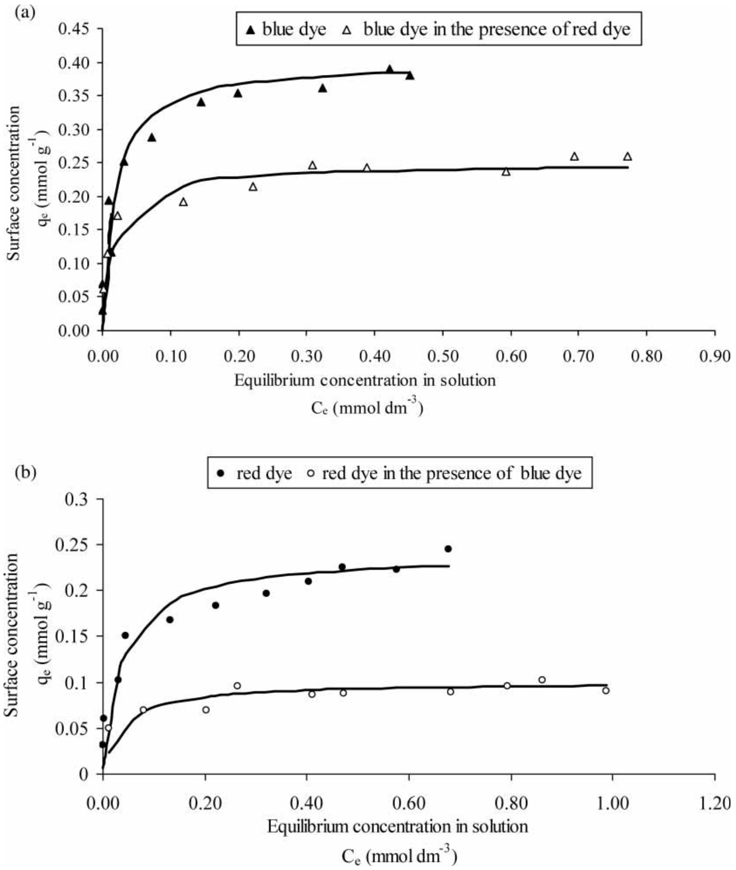

Figure 3. Adsorption isotherms of reactive dyes by activated carbon: (a) reactive blue in single and bi-solute solutions. (b) red dye in single and bi-solution solution. Mass of carbon: 0.200 g, volume of solution: 100.0 cm^3. pH: 5–6. Dyes concentration range in single and bi-solute solutions: $0–1.2 \times 10^{-3}$ mol dm^{-3}. Temperature: 25($\pm$1)°C. Filled and empty points represent experimental data, lines represent Langmuir model (equation (4)).

Or in the linear from:

$$\frac{C_e}{q_e} = \frac{1}{K_L Q_{\max}} + \frac{C_e}{Q_{\max}} \tag{5}$$

Where: C_e is the equilibrium concentration of the dye in solution (mol dm^{-3}); q_e is the surface concentration of the dye at equilibrium (mol g^{-1}); $Q_{\max}$ is the amount of dye adsorbed at complete monolayer coverage (mol g^{-1}); K_L (dm^3 mmol^{-1}) is a constant that relates to the heat of adsorption (28).

The Freundlich model has the following form (34)

$$q_e = k_F C_e^n \tag{6}$$

Or in the linear from:

$$\log q_e = \log k_F + n \log C_e \tag{7}$$

Where: K_F (mmol g^{-1}) (mmol dm^{-3})$^{-n}$ represents the adsorption capacity when dye equilibrium concentration and $n-$represents the degree of dependence of adsorption with equilibrium concentration.

Three-Parameter Model

Redlich–Peterson model has three parameters, K_R (dm^3 g^{-1}), b_R (mmol dm^{-3})$^{-\beta}$, and $\beta-$.The parameter (β) ranges between 0 and 1 (4).

$$q_e = \frac{K_R C_e}{1 + b_R C_e^{\beta}} \tag{8}$$

This isotherm describes the adsorption on heterogeneous surfaces, as it contains the heterogeneity factor β. This model can be reduced to the Langmuir isotherm (equation (4)) when $\beta = 1$ and replacing K_R and b_R by the Langmuir constants $Q_{\max} K_L$ and K_L respectively (31).

The parameters of the models employed (equations: (4), (6), and (8) were obtained using the nonlinear regression method. The parameters of the Langmuir and Freundlich models can be easily obtained using either the simple linear regression method or a non-linear regression method (35). The Redlich–Peterson equation cannot be linearized, therefore, a non-linear regression method is necessary. In a recent study, Kumar and Sivanesan have indicated that non-linear regression methods are more appropriate than simple linear regression methods when correlating the adsorption data to the Langmuir, Freundlich, and the Redlich-Peterson models (35). The model parameters were determined by minimizing the respective coefficient of determination between experimental data and models using Microsoft

Excel. In the present work, the coefficient of determination r^2 was used to determine the best-fit model:

$$r^2 = \frac{\sum (q_{\text{cal}} - \overline{q}_{\text{exp}})^2}{\sum (q_{\text{cal}} - \overline{q}_{\text{exp}})^2 + \sum (q_{\text{cal}} - q_{\text{exp}})^2} \tag{9}$$

where: q_{cal} is the surface concentration obtained from the model; q_{exp} is the experimental value of the surface concentration, and $\bar{q}_{\text{exp}}$ is the average of q_{e} values. The obtained parameters for the three models along with (r^2) values are presented in Table 3.

Langmuir Model

This model assumes that the surface has a limited number of active sites and the adsorption of the solute continues until the surface sites are occupied and the interaction between adsorbed molecules is neglected. The correlation of adsorption data of both the dyes from single-solute solutions to the Langmuir model was fairly good with r^2 values of 0.967 and 0.955 for blue and red dye respectively. As shown in Table 3, the maximum adsorption values of the dyes are: 0.42 and 0.25 mmol g^{-1} for blue and red dye respectively. Gan and co-workers have studied the adsorption of the same red dye used in this study on a commercial activated carbon and they reported a maximum adsorption value of 0.28 mmol g^{-1} (36). K_L, represents the equilibrium adsorption constant for the adsorption reaction and is the ratio between adsorption rates constant to the desorption rate constant. Higher values of K_L indicate that the solute favorably transfers from the solution to attach to the adsorbent surface. By comparing the values of K_L of the two dyes, it can be concluded that the adsorption of the blue dye ($K_L = 55.2$) is highly favorable compared to the red dye ($K_L = 23.0$). The fraction of the carbon surface that is occupied by dye molecules (θ) can be calculated from the

Table 3. Model parameters obtained from fitting the experimental equilibrium data with various isotherm models

Model	C_e range (mmol/dm^3)	Model parameters			r^2
Blue dye					
Langmuir	0–0.45	$K_L = 55.2$	$Q_{\max} = 0.42$		0.967
Freundlich	0–0.45	$K_F = 0.47$	$n = 0.21$		0.954
Redlich-Peterson	0–0.45	$K_R = 55.0$	$b_r = 84.3$	$\beta = 0.66$	0.912
Red dye					
Langmuir	0–0.68	$K_L = 23.0$	$Q_{\max} = 0.25$		0.955
Freundlich	0–0.68	$K_F = 0.27$	$n = 0.25$		0.904
Redlich-Peterson	0–0.68	$K_R = 18.0$	$b_r = 61.5$	$\beta = 0.79$	0.962

amount of dye adsorbed and the surface area occupied by one dye molecule (σ) using the following equation (25, 37)

$$\theta = \frac{Q_{\max} N \sigma 10^{-20}}{S_{\mathrm{BET}}} \tag{10}$$

Where: θ represents the fraction of the surface that is occupied by dye molecules at saturation; $Q_{\max}$ (mol g^{-1}) is the amount of dye adsorbed at saturation as obtained from the Langmuir model; σ ($\mathring{A}^2$/molecule) is the surface area occupied by one molecule; N is the Avogadro's number (6.022×10^{23}); S_{BET} specific surface area of the adsorbent as calculated from N_2 adsorption method ($820\ m^2/g$). When $\theta = 1$, the surface is fully occupied with the adsorbate molecules. McClellan and Harnsberger have proposed an empirical relationship that can be used for the estimation of σ for organic molecules adsorbed on activated carbon (38)

$$\sigma(\overset{o}{\mathrm{A}}\,A^2/\mathrm{molecule}) = 1.091 \times 10^{16} \left(\frac{MW}{\rho N}\right)^{2/3} \tag{11}$$

Where: σ is the surface area occupied by the adsorbate molecule ($\mathring{A}^2$); MW is the molar mass of the adsorbed molecule (g/mol); ρ is the adsorbate density (g/cm^3). The bulk densities of dyes are 0.415 and 0.445 g/cm^3 for red and blue dye respectively. Accordingly, the values of (θ) are 0.45 and 0.69 for red and blue respectively. The values of θ indicate that the formation of a complete molecular layer was not achieved at saturation for both dyes and a large fraction of the surface remains unoccupied particularly in the case of the red dye. For both dyes, the formation of a complete mono-layer is not possible as the dye molecules are relatively large and can not access some of the micropores which contain about 87% of the total surface area of the adsorbent. In the case of the red dye adsorption, 55% of the total surface area remained unoccupied. The surface of the activated carbon is occupied more by blue dye molecules ($\theta = 0.69$) compared to the red dye molecules ($\theta = 0.45$) due to the higher extent of adsorption.

Freundlich Model

The parameters of the Freundlich model (K_F and n) can indicate the nature of the dye adsorption, i.e., favorable or unfavorable under the studied experimental conditions (39). K_F is an indicator of adsorption capacity and n is an indicator of surface heterogeneity and adsorption favorability (25). A greater value of K_F indicates a higher adsorption extent for a given adsorbate. Lower values of n ($n < 1$) indicate that the adsorption process is favorable over the entire concentration range, while higher values of n ($n > 1$) indicates that the adsorption process is unfavorable under the studied concentration range (39). Lower values of n also reflect the high heterogeneity of the adsorbent surface (25). The Freundlich model parameters and r^2 values are presented in Table 3. As shown in Table 3, the values of r^2 indicate that the Freundlich model showed better correlation to the adsorption data of the blue dye compared to the red dye data over the entire concentration range. The adsorption intensity of the blue dye is almost twice than that of the red dye as inferred from the obtained values of K_F, 0.47 and 0.27 for the blue and the red dye respectively. K_F is a good indicator for the intensity of solute adsorption. The high adsorption extent of the blue dye compared to the red dye was also evident from the values of $Q_{\max}$ of the Langmuir model. The n values for both adsorption systems were less than unity which reflects the favorable adsorption of both dyes. Furthermore, the surface of the activated carbon may be highly heterogeneous and the energies of active sites highly variable as the values of n are much less than unity (25, 31).

Redlich-Peterson Model and the Heterogeneity Factor (β)

The Redlich-Peterson model is of interest as it can be used to estimate the heterogeneity factor (β) of the adsorbent surface. The model parameters and r^2 values are presented in Table 3. The values of r^2 indicate that the adsorption data for the red dye show better correlation to this model compared to the blue dye data over the entire concentration range. This model appears to validate the result of the Freundlich model as β values for both adsorption systems are less than unity which reflects the heterogeneity of the surface (31). If β was equal to unity, then the Redlich-Peterson equation reduces to the Langmuir model which assumes a homogenous surface of the adsorbent.

Mechanisms of Dyes Interaction with Activated Carbon

The molecular dimensions of the dyes molecules (assuming a planar geometry of molecules) were calculated using the semiempirical molecular orbital method (PM3 method) (14). The molecular dimensions were calculated as 1.92 and 1.25 for the red dye and 2.20 and 1.10 nm for the blue dye. Comparing the plane-molecular areas of dyes molecules (which can be computed from their corresponding dimensions) with the surface areas occupied by the molecules (σ), the geometry of the adsorbed dyes can be recognized. Table 4 contains the values of the areas occupied by adsorbed dyes and their plane-molecular areas.

There are two possible mechanisms for the dyes to adsorb on the carbon surface:

a) the plane of the dye molecule is parallel to the surface (in this case the dye would occupy largest possible area)

Table 4. The plane-molecular areas of dyes and the areas occupied by adsorbed dyes molecules as obtained from equation 11

Dye	Molecular dimensions (nm)[a]	Plane-molecular area (Å^2)[b]	Occupied area (Å^2)
Blue	2.20 and 1.10	242.0	224.0
Red	1.92 and 1.25	240.0	245.0

[a] Obtained from the Hyperchem program.
[b] Obtained from the dimensions of the molecules.
[c] Obtained from equation 11.

b) the plane of the dye molecule is perpendicular to the surface of the adsorbent (in this case a smaller area would be occupied).

As shown in Table 4, the plane-molecular areas of dyes are very close (particularly in the case of red dye) to those obtained from equation (11) which would strongly indicate that the dyes adsorb according to the first mechanism. Such an adsorption process could happen when the polyheterocycles and benzene rings of the dyes orientate parallel to the adsorbent surface with the planar face of dyes molecules (shown in Fig. 1) facing the solid surface. Diffusion of reactive dyes within the mesopores (average pore diameter 1.8 nm) is possible. Assuming that the entrance of the micropores is circular in shape, then the area of the entrance is equal to 255 Å^2. As shown in Table 4, the estimated molecular areas of the dyes are 242 and 240 Å^2 which indicate that the dyes can access the micropores. Large molecules like dyes can also adsorb on the external surface area and diffuse inside the mesopores (pore diameter: 2–50 nm) more effectively than diffusion through the micropores of the adsorbent. In a similar study, Nakagawa et al., 2004, have shown that mesoporous activated carbons were more effective for removing large size reactive dye molecules compared to microporous activated carbons (40).

Reactive dyes are capable of interacting with the surface of activated carbon. Interactions occur via several mechanisms. These interactions can be divided into weak and strong interactions. The weak interactions occur due to the presence of van der Waals forces, while strong interactions occur due to the following processes (26).

a. Electrostatic interaction between negatively charged reactive dyes (due to the presence of SO_3^- groups) and positively charged carbon sites. This mechanism is possible because the adsorption isotherms were carried out at pH range: 5.0–5.5 and at that pH reactive dyes and activated carbon are differently charged.
b. Hydrogen bonding interactions are possible between oxygen and nitrogen-containing functional groups of both reactive dyes and the activated

carbon. As indicated from the chemical structures of both dyes, there are a number of functional groups that can induce hydrogen-bonding with the surface of activated carbon and these include: -NH_2, -C=O, and -S=O groups. Furthermore, activated carbon has a number of functional groups that can induce hydrogen-bonding with dye molecules, among them: carboxylic and phenolic groups.

c. Hydrophopic-hydrophopic interactions between the hydrophobic part of the dyes molecules and the hydrophobic regions of the activated carbon within graphitic regions (26). This mechanism is possible because both the dyes have hydrophobic characteristics as indicated from the percentage of carbon atoms compared to the oxygen and the nitrogen atoms.

The combination of these interactions in reactive dyes allow for the adsorption on activated carbon. In this particular case, the first and second mechanisms would have a minor contribution in dye adsorption due to the relatively low density of the adsorbent surface functional groups (0.45 group/nm^2). For example, the occupied surface areas of the blue and the red dye as obtained from equation 11 are 2.24 and 2.45 nm^2 respectively. Accordingly, the number of surface functional groups that would interact with one dye molecule is approximately one. It is unlikely that a single surface functional group on the activated carbon is capable of attracting a large dye molecule.

Both dyes have similar molecular dimensions and similar chemical functionalities as shown in Fig. 1; however, the blue dye showed a high extent of adsorption compared to the red dye. The variation in the extent of dye adsorption can be correlated to their *n*-octanol/water partition coefficients (K_{OW}) or their hydrophobicity. The *n*-octanol/water partition coefficient provides a relatively convenient means of predicting the distribution of hydrophobic organic molecules (like dyes and pesticides) between the dissolved state in water and the adsorbed state on hydrophobic surfaces. A solute of high K_{OW} value has a high hydrophobicity and has a high tendency to leave water and adsorb on the hydrophobic surface of activated carbon. The matrix of activated carbon is mainly hydrophobic because of the high percentage of carbon (83%) compare to oxygen (7.3%) as indicated from the elemental analysis provided by the manufacturer. The K_{OW} values are 1.2×10^3 and 1.8×10^4 for the red and the blue dye respectively. Reactive blue is more hydrophopic in character (higher K_{OW} value) than the red dye and this hydrophobicity may have increased the extent of the adsorption extent on the hydrophobic surface of activated carbon. Kiso and co-workers have shown that adsorption properties were controlled by both hydrophobicity (which is related to the *n*-octanol/water partition coefficient) and the molecular shape of the solute (41). Based on this, it is highly possible that the dominant mechanism of the dye interaction with activated carbon is the hydrophobic-hydrophobic mechanism.

Competitive Adsorption of Reactive Dyes from Solution

The adsorption of reactive dyes from a bi-solute solution was investigated in this study. It can be noted from Fig: 3a and 3b, that the extent of adsorption of both dyes in bi-solute solution was lower than from single solute solutions. This confirms that there was competition between the dye molecules for the surface active sites. The extent of competition between dyes can be presented by the ratio of the adsorption capacity for one dye in the presence of the other dye, $Q_{\text{bi-solute}}$, to the adsorption capacity for the same dye from single solute solution ($Q_{\text{single-solute}}$):

$$\text{Competition factor (CF)} = \frac{Q_{\text{bi-solute}}}{Q_{\text{sin gle-solute}}} \tag{12}$$

Positive competition is present if the competitive factor (CF) is higher than unity; the adsorption is enhanced in this case by the presence of the other solute. No competition between solutes is expected if CF is equal to unity. The more common case is that the CF is less than unity which indicates that the adsorption capacity of the solute is suppressed in the presence of the other solute. The adsorption data of the reactive dyes from the bi-solute solution was correlated to the Langmuir model (equation (4) and the competitive-Langmuir model (equations (13) and (14)). The competitive-Langmuir model has been developed for competitive multisolute adsorption (11, 12). This model assumes a homogeneous surface with respect to the energy of adsorption, no interaction between adsorbed species, and that all sites are equally available to all adsorbed species (11). For example, for two solutes 1 and 2, the adsorption capacity of solute 1 in the presence of solute 2 can be calculated from the competitive-Langmuir model as follows:

$$q_{e1} = \frac{Q_{\max 1} K_{L1} C_{e1}}{1 + K_{L1} C_{e1} + K_{L2} C_{e2}} \tag{13}$$

The adsorption capacity of solute 2 in the presence of solute 1 can similarly be obtained:

$$q_{e2} = \frac{Q_{\max 2} K_{L2} C_{e2}}{1 + K_{L1} C_{e1} + K_{L2} C_{e2}} \tag{14}$$

Where: q_{e1}, q_{e2}, $Q_{\max 1}$, $Q_{\max 2}$, C_{e1}, C_{e2}, K_{L1} and K_{L2} are the surface concentration of solute 1 and 2 at equilibrium respectively, the saturation values of solute 1 and 2 respectively, the remaining concentration of solute 1 and 2 in solution respectively, and the Langmuir equilibrium constant for solute 1 and 2 respectively. In this case, solute 1 represents blue dye, while solute 2 represents red dye. From the theoretical point of view, the values of the equilibrium constants (K_{L1} and K_{L2}) should be similar to those obtained from single-solute systems as the equilibrium constant is a temperature dependant parameter and therefore should follow the vant Hoff equation (28):

$$K_L = Ae^{-\Delta H/RT} \tag{15}$$

Where: A and ΔH are vant Hoff constant and enthalpy of adsorption process. Table 5 summarized the results of fitting the adsorption data of the dyes in the binary system using equations (13) and (14). For comparison purposes, the adsorption data of both dyes from the single-solute solution are also included in Table 5. Figure 4 illustrates the fitting of the adsorption isotherms of both dyes in the bi-solute system using the Langmuir and competitive-Langmuir models.

As shown in Table 5, the competition factors for both dyes were less than unity which indicates that the extent of adsorption for both dyes from the bi-solute solution is considerably reduced. The competition factors for both dyes are 0.62 and 0.40 for the blue and the red dye respectively. The reduction in adsorption of the red dye was higher compared to the blue dye, and this was anticipated from the lower competition factor of the former dye.

The large reduction in red dye adsorption can be attributed to the high affinity of blue dye to the carbon surface as indicated from the adsorption isotherm of single-solute systems. As indicated from Tables 3 and 5, the adsorption value ($Q_{\max}$) of blue dye is about 1.7 times higher than the adsorption value of the red dye. Competitive adsorption data of the dyes correlated well to the Langmuir model (equation (4)), over the entire concentration range. The equilibrium adsorption constants (K_L) for the dyes in the binary system were relatively similar to the equilibrium values obtained from single-solute systems as indicated in Table 5. For single-solute systems, the equilibrium adsorption constants were 55.2 and 23.0 for blue and red dye respectively, in the bi-solute system, the equilibrium constants were similar at 51.0 and 26.4 for blue and red dye respectively. As indicated in Table 5, the maximum adsorption capacities of the dyes in the bi-solute system (as obtained from the Langmuir equation) were 0.26 and 0.10 mmol g^{-1}. It is interesting to note the magnitude of the adsorption capacities (in mg g^{-1} units) of the dyes from single and bi-solute systems. The adsorption capacities of the dyes from single and binary systems (in mg g^{-1} units) are: 330.0, 204.4, 210.4, 84.2 mg g^{-1} for: blue dye alone; blue dye in the presence of the red dye; the red dye alone; the red dye in the presence of the blue dye respectively. The combined adsorption capacity of activated carbon for both dyes in the mixture is 288.6 mg g^{-1}. This value is considerably less than the adsorption value of the blue dye adsorbed from the single-solute system (330.0 mg g^{-1}). This reflects the significant reduction in the efficiency of activated carbon for the adsorption of a dye mixture of dyes and also the high degree of competition between the adsorbing species. The coefficient of determination (r^2) indicates that the adsorption isotherm data of reactive

Table 5. Parameter values from fitting the competitive adsorption data with the Langmuir and competitive-Langmuir models

	Langmuir model				Competitive-Langmuir model						
System	$Q_{\max}$	K_L	C_e range	r^2	$Q_{\max 1}$	K_{L1}	$Q_{\max 2}$	K_{L2}	C_e range	r^2	Competition factor (CF)[a]
Reactive blue	0.42	55.2	0–0.45	0.967							
Reactive blue (with reactive red)	0.26	51.0	0–0.77	0.903	0.43	55.2		23.0	0–0.77	0.83	0.62
Reactive red	0.25	23.0	0–0.68	0.955							
Reactive red (with reactive blue)	0.10	26.4	0–0.98	0.810		55.2	0.19	23.0	0–0.98	0.41	0.40

[a] CF value was calculated by dividing the adsorption capacity of dye from bi-solute solution which obtained from the Langmuir model (equation (4)) by the adsorption capacity of the dye when adsorbed alone under the same experimental conditions.

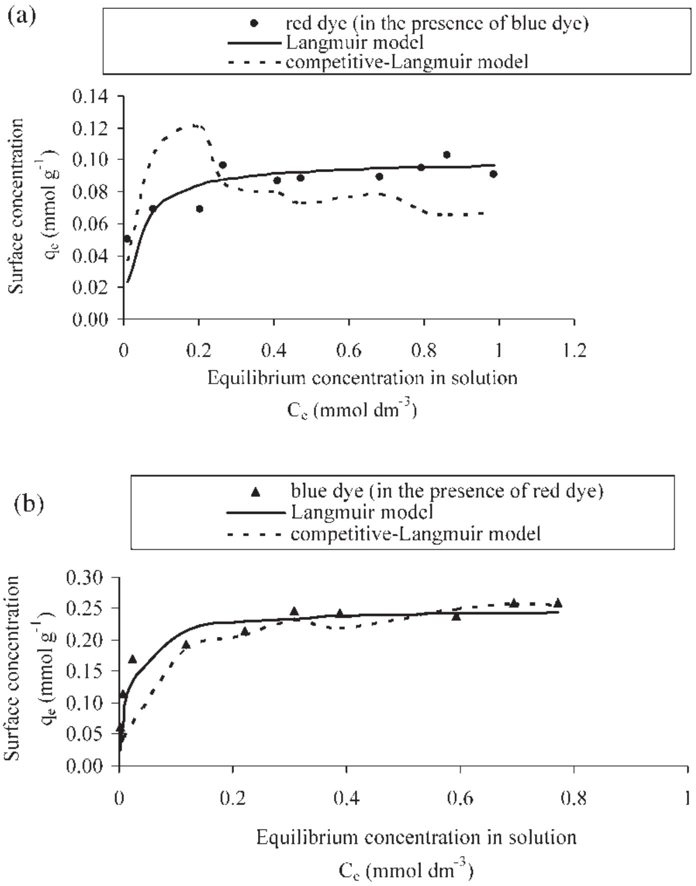

Figure 4. Adsorption isotherm of (a) red dye in the presence of blue dye and (b) blue dye in the presence of red dye.

dyes from the single-solute systems correlated better to the Langmuir model compared to the data of the bi-solute system. This can be attributed to the competition between the dyes in the solution and possible interaction between the dyes in the adsorbed phase, such interactions are not considered in the Langmuir isotherm (equation (4)). Accordingly, this may limit the application of the model to the bi-solute adsorption systems.

The adsorption data of a binary system were also fitted to the competitive-Langmuir model (equations (13) and (14)). When applying this model, the values of the equilibrium constants of dyes were assumed to be constant and equal to the values obtained from the single-solute systems. The competitive-Langmuir model appears to have a limited application to the this adsorption system. As shown in Fig. 4a and b, the model shows poor correlation for the adsorption isotherm of red dye in the presence of the blue dye, the coefficient of determination was 0.41 as shown in Table 5. Moreover, the adsorption capacity of the red dye ($Q_{\max2}$) as predicted from the competitive-Langmuir model (equation (14)) is 0.19 mmol g^{-1}, this value is almost double than the one predicted from simple Langmuir equation (0.10) mmol g^{-1}) as shown in Table 5. Even though, Equation (13) gave a better graphical presentation for the adsorption isotherm of blue dye ($r^2 = 0.83$), the model gives an over-estimation for $Q_{\max1}$ of blue dye. The value of $Q_{\max1}$, is obtained from the fitting of equation (13) to the adsorption isotherm over the equilibrium concentration range (0–0.77 mmol dm^{-3}) is 0.43 mmol g^{-1}. The magnitude of the adsorption capacity of the blue dye, obtained from the Langmuir isotherm (0.26 mmol g^{-1}) is more reasonable. Generally, the results of the competitive-Langmuir model indicate that this model has a limited application to the bi-solute adsorption systems in this study. The poor presentation of the competitive-Langmuir model (equations (13) and (14)) for dyes isotherms can be attributed to the fact that this model has the same basic assumptions of the Langmuir model, namely constant energy of adsorption, no interaction between solutes, and equal independent competition between species; these appear not to hold true in this application. Furthermore, Choy and co-workers reported a limited application of the competitive-Langmuir models for representing the binary adsorption systems of acid dyes (12).

Desorption of Reactive Dyes from the Surface of Activated Carbon

Relatively few studies have considered the desorption and regeneration of dyes using water and other organic solvents (13, 33, 42, 43). The extent of irreversible adsorption (or desorption extent) of reactive dyes from the surface of activated carbon was studied using water as a solvent. The method of analysis of desorption results used in this study was adopted from the work of Chatzopoulos and co-workers (34). The total amount of dye adsorbed is equal to the amount of dye reversibly adsorbed and irreversibly adsorbed:

$$q_e = q_{e,rev} + q_{e,irrev} \tag{16}$$

Where: q_e is the total amount of adsorbed dye (mol g^{-1}); $q_{e,rev}$ is the amount of reversibly adsorbed dye; and $q_{e,irrev}$ is the amount of irreversibly adsorbed dye. From a theoretical viewpoint, the adsorption process is completely reversible if all adsorbed dye molecules were desorbed during the course of desorptions; however, this not likely to happen due to the heterogeneity of the carbon surface, where a high degree of interaction is possible between some dye molecules and some sites of higher energy. This will leave some dye molecules strongly attached to the surface which will not desorb. During desorption, some molecules which are reversibly adsorbed will leave the surface until equilibrium is established between dye concentration

$C_{\acute{e}}$ in solution and the remaining surface concentration of the reversibly adsorbed dye $q_{e,rev}$. $C_{\acute{e}}$ and $q_{e,\mathrm{rev}}$ can be related to the Langmuir equation (equation (4)) as follows:

$$q_{e,rev} = \frac{K_L Q_{\max} C_{\acute{e}}}{1 + L_L C_{\acute{e}}} \tag{17}$$

The adsorption parameters (K_L and $Q_{\max}$) for both dyes were reported in Table 3. Accordingly, the values of $q_{e,rev}$ can be calculated from equation (17) when $C_{\acute{e}}$ values are known. To calculate the total amount of reversibly adsorbed molecules $q_{\mathrm{total,rev}}$ (the amount remaining on the surface and the amount desorbed), equation 18 is used:

$$q_{total,rev} = q_{e,rev} + \frac{VC_{\acute{e}}}{m} \tag{18}$$

Where: V is the volume of the desorption solution (dm^3) and m is the mass of the adsorbent. The fraction of reversible adsorption of dyes (FRA) can be obtained from the following relation:

$$\text{Fraction of reversible adsorption (FRA)} = \frac{q_{total,rev}}{q_e} \tag{19}$$

It is noted that the value of FRA is also equal to the fraction of dye desorbed from the carbon by water. The fraction of reversible adsorption (FRA) of reactive dyes was estimated at different dye surface concentrations with the results depicted in Fig. 5.

As shown in Fig. 5, the values of FRA of the blue dye were much higher than that of the red dye at the studied surface concentration, which extends from low surface coverage to saturation (0.02–0.45 mmol g^{-1}). As indicated in Fig. 5, the FRA value of the blue dye is approximately 0.3 (i.e., 30% of the adsorbed dye was desorbed by water and 70% remained on the surface) at surface concentration range 0.4–0.45 mmol g^{-1}. The FRA values are very small at lower initial surface concentration (less than 0.2 mmol g^{-1}); this is due to lower surface coverage, only the high-energy active sites were occupied. Due to the high interaction of dyes with these high-energy active sites, adsorption should be very strong. However, at a higher surface coverage, most active sites would be occupied and the desorption of dyes from the lower-energy sites is more probable (34). Over the entire surface concentration of red dye (0.02–0.23 mmol g^{-1}), the values of FRA were modest, with the maximum value of 0.05 obtained (at the maximum surface concentration 0.23 mmol g^{-1}). From the data presented in Fig.5, the nature of the binding of the reactive dyes with activated carbon can be determined. The lower values FRA for the red dye indicate that chemical interactions are occurring to a greater extent. For the blue dye, the lower values of FRA over the surface concentration range (0.02–0.2 mmol g^{-1}) indicate that chemical interaction is the sole mechanism, while at surface concentrations higher than 0.2 mmol g^{-1} the magnitude of

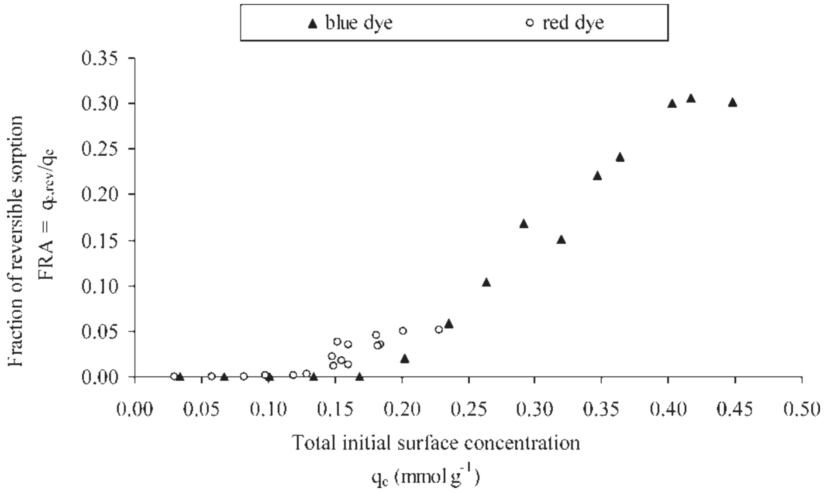

Figure 5. Fraction of reversible adsorption (FRA) of dyes as a function of the total initial surface concentration (q_e).

FRA increases thus indicating that weak physical interaction occurs to some extent. In general, the values of FRA are small for both dyes, reflecting the high affinity of dyes with the carbon surface. The high extent of interaction between reactive dyes and the hydrophobic surface of activated carbon can be attributed to the high hydrophobic-hydrophobic interactions, inferred from the high hydrophobicity of dyes as indicated from their high K_{OW} values.

CONCLUSION

H-type activated carbon has a high adsorption capacity for reactive dyes. The adsorption extent of reactive dyes from a single-solute solution was high, 0.42 mmol/g and 0.25 mmol/g for the blue and the red dye respectively. In binary solution, dyes showed a high competition for active sites and the obtained adsorption capacities were reduced to 0.26 and 0.1 mmol/g for the blue and the red dye respectively. Experimental data indicated that the formation of a complete mono-layer was not achieved and the fraction of the surface coverage was 0.69 and 0.45 for the blue and the red dye respectively. Interactions of the dyes with activated carbon occur via hydrophobic-hydrophobic interactions between the hydrophobic part dyes molecules, and the hydrophobic part of the activated carbon. The competitive-Langmuir model was found to have a limited application for presenting binary adsorption systems. For the blue dye at the initial surface concentration of 0.45 mmol/g, 30% of the adsorbed was desorbed using water. For surface concentrations less than 0.2 mmol/g, desorption was insignificant. For the reactive red dye, desorption was insignificant at the initial surface concentration range: 0.02–0.23 mmol/g. The poor desorption of the reactive dyes from the activated carbon indicates that a significant fraction of the adsorbed dyes were strongly attached to the carbon surface.

REFERENCES

1. Robinson, T., McMullan, G., Marchant, R., and Nigam, P. (2001) Remediation of dyes in textile effluent: a critical review on current treatment technologies with a proposed alternative. *Bioresource Technology*, 77: 247.
2. Mottaleb, M. and Littlejohn, D. (2001) Application of an HPLC-FTIR modified thermospary interface for analysis of dye samples. *Analytical Science*, 17: 429.
3. Al-Degs, Y., El-Barghouthi, M., Khraisheh, M., Ahmad, M., and Allen, S. (2004) Effect of surface area, micropores, secondary micropores and mesopores volumes of activated carbons on reactive dyes adsorption from solution. *Separation Science and Technology*, 39: 97.
4. Wang, S., Boyjoo, Y., Choueib, A., and Zhu, Z. (2005) Removal of dyes from solution using fly ash and red mud. *Water Research*, 39: 129.
5. Órfão, J., Silva, A., Pereira, J., Barata, S., Fonseca, I., Faria, P., and Pereira, M. (2006) Adsorption of a reactive dye on chemically modified activated carbons—Influence of pH. *Journal of Colloid and Interface Science*, 296: 480.
6. Yang, X. and Al-Duri, B. (2001) Application of branched pore diffusion model in the adsorption of reactive dyes on activated carbon. *Chemical Engineering Journal*, 83: 15.
7. Vandevivere, P., Bianchi, R., and Verstraete, W. (1998) Review: Treatment and reuse of wastewater from the textile wet-processing industry: Review of emerging technologies. *J. Chem. Technol. Biotechnol.*, 72: 289.
8. Faria, P., Órfão, J., and Pereira, M. (2004) Adsorption of anionic and cationic dyes on activated carbons with different surface chemistries. *Water Research*, 38: 2043.
9. Janoš, P., Buchtová, H., and Rýznarová, M. (2003) Sorption of dyes from aqueous solutions onto fly ash. *Water Research*, 37: 4938.
10. Crini, G. (2006) Non-conventional low-cost adsorbents for dye removal: A review. *Bioresource Technology*, 97: 1061.
11. Allen, S., Mckay, G., and Porter, J. (2004) Adsorption isotherm models for basic dye adsorption by peat in single and binary component systems. *Journal of Colloid and Interface Science*, 280: 322.
12. Choy, K., Mckay, M., and Porter, J. (1999) Sorption of acid dyes from effluents using activated carbon. *Resources, Conservation and Recycling*, 27: 57.
13. Tanthapanichakoon, W., Ariyadejwanich, P., Japthong, P., Nakagawa, K., Mukai, S., and Tamon, H. (2005) Adsorption–desorption characteristics of phenol and reactive dyes from aqueous solution on mesoporous activated carbon prepared from waste tires. *Water Research*, 39: 1347.
14. Stewart, J. (1989) Optimization of parameters for semiempirical methods I. Method. *Journal of Computational Chemistry*, 10: 209.
15. Boehm, H. (1994) Some aspects of the surface chemistry of carbon blacks and other carbons. *Carbon*, 32: 759.
16. Güzel, F. and Tez, Z. (1993) The characterization of the micropore structure of some activated carbon of plant origin by N_2 and CO_2 adsorption. *Separation Science and Technology*, 28: 1609.

17. Al-Duri, B., Khader, K., and Mckay, G. (1992) Prediction of binary compound isotherm for adsorption on heterogeneous surfaces. *J. Chem. Tech. Biotechnol.*, 53: 345.
18. Berthod, A. and Carda-Broch, S. (2004) Review: Determination of liquid–liquid partition coefficients by separation methods. *Journal of Chromatography A*, 1037: 3.
19. Chun, Y., Sheng, G., Chiou, C., and Xing, B. (2004) Compositions and sorptive properties of crop residue-derived chars. *Environ. Sci. Technol.*, 38: 4649.
20. Leon, Y., Leon, C., Solar, J., Calemma, V., and Radovic, L. (1992) Evidence for the protonation of basal plane sites on carbon. *Carbon*, 30: 797.
21. Mattson, J. and Mark, H. (1971) *Activated Carbon: Surface Chemistry and Adsorption from Solution*; Marcel Dekker: New York.
22. Mazet, M., Farkhani, B., and Baudu, M. (1994) Influence of heat or chemical treatment of activated carbon onto the adsorption of organic compounds. *Water Research*, 28: 1609.
23. Al-Degs, Y., Khraisheh, M., Allen, S., and Ahmad, M. (2000) Effect of carbon surface chemistry on the removal of reactive dyes from textile effluents. *Water Research*, 34: 927.
24. Gregg, S. and Sing, K. (1982) *Adsorption, Surface Area and Porosity*, 2nd Ed.; Academic Press.
25. Haghseresht, H. and Lu, G. (1998) Adsorption characteristics of phenolic compounds onto coal-rejected-derived adsorbents. *Energy and Fuels*, 12: 1100.
26. Newcombe, G. and Drikas, M. (1997) Adsorption of NOM activated carbon: electrostatic and NON-electrostatic effects. *Carbon*, 35: 1239.
27. El-Sheikh, A., Newman, A., Al-Daffaee, H., Phull, S., and Cresswell, N. (2004) Characterization of activated carbon prepared from a single cultivar of Jordanian Olive stones by chemical and physicochemical techniques. *Journal of Analytical and Applied Pyrolysis*, 71: 151.
28. Ruthven, D. (1984) *Principles of Adsorption and Adsorption Processes*; John Wiley and Sons: NJ.
29. Lillo-Ródenas, M., Fletcher, A., Thomas, K., Cazorla-Amoró, D., and Linares-Solano, A. (2006) Competitive adsorption of a benzene–toluene mixture on activated carbons at low concentration. *Carbon*, 44: 1455.
30. Giles, C. and Smith, D. (1974) General treatment and classification of the solute sorption isotherms. *J. Colloid Interface Science*, 47: 755.
31. Yang, X. and Al-Duri, B. (2005) Kinetic modeling of liquid-phase adsorption of reactive dyes on activated carbon. *J. Colloid Interface Science*, 287: 25.
32. Moreira, R., Kuhnen, N., and Peruch, M. (1998) Adsorption of reactive dyes onto granular activated carbon. *Latin American Applied Research*, 28: 37.
33. Walker, G., Hansen, L., Hanna, J., and Allen, S. (2003) Kinetics of a reactive dye adsorption onto dolomite sorbents. *Water Research*, 37: 2081.
34. Chatzopoulos, D., Varma, A., and Irvine, R. (1993) Activated carbon adsorption and desorption of toluene in the aqueous phase. *AIChE Journal*, 39: 2027.
35. Kumar, K. and Sivanesan, S. (2006) Isotherm parameters for basic dyes onto activated carbon: Comparison of linear and non-linear method. *Journal of Hazardous Materials*, B129: 147.
36. Gan, Q., Allen, S., and Matthews, R. (2004) Activation of waste MDF sawdust charcoal and its reactive dye adsorption characteristics. *Waste Management*, 24: 841.

37. Gusler, G., Browne, T., and Cohen, Y. (1993) Sorption of organics from aqueous solution onto polymeric resins. *Industrial & Engineering Chemistry Research*, 32: 2727.
38. McClellan, A. and Harnsberger, H. (1967) Cross-sectional areas of molecules adsorbed on solid surfaces. *Journal of Colloid and Interface Science*, 23: 577.
39. Frimmel, F. and Huber, L. (1996) Influence of humic substances on the aquatic sorption of heavy metals on defined minerals phases. *Environment International*, 22: 507.
40. Nakagawa, K., Namba, A., Mukai, S., Tamon, H., Ariyadejwanich, P., and Tanthapanichakoon, W. (2004) Adsorption of phenol and reactive dye from aqueous solution on activated carbons derived from solid wastes. *Water Research*, 38: 1791.
41. Kiso, Y., Sugiura, Y., Kitao, T., and Nishimura, K. (2001) Effects of hydrophobicity and molecular size on rejection of aromatic pesticides with nanofiltration membranes. *Journal of Membrane Science*, 192: 1.
42. Mittal, A. and Venkobachar, C. (1993) Sorption and desorption of dyes by sulfonated coal. *Journal of Environmental Engineering*, 119: 366.
43. McKay, G., Ramprasad, G., and Mowli, P. (1987) Desorption and regeneration of dye colours from low-cost materials. *Water Research*, 21: 375.